



HAL
open science

Sea Level Interannual Variability Along the West Coast of India

Iyyappan Suresh, Jérôme Vialard, Matthieu Lengaigne, Takeshi Izumo,
Vallivattathillam Parvathi, Pillathu Moolayil Muraleedharan

► **To cite this version:**

Iyyappan Suresh, Jérôme Vialard, Matthieu Lengaigne, Takeshi Izumo, Vallivattathillam Parvathi, et al.. Sea Level Interannual Variability Along the West Coast of India. *Geophysical Research Letters*, 2018, 45 (22), pp.12,440-12,448. 10.1029/2018GL080972 . hal-02190654

HAL Id: hal-02190654

<https://hal.science/hal-02190654>

Submitted on 18 Nov 2021

HAL is a multi-disciplinary open access archive for the deposit and dissemination of scientific research documents, whether they are published or not. The documents may come from teaching and research institutions in France or abroad, or from public or private research centers.

L'archive ouverte pluridisciplinaire **HAL**, est destinée au dépôt et à la diffusion de documents scientifiques de niveau recherche, publiés ou non, émanant des établissements d'enseignement et de recherche français ou étrangers, des laboratoires publics ou privés.

Copyright

RESEARCH LETTER

10.1029/2018GL080972

Key Points:

- Positive Indian Ocean Dipoles induce positive (negative) sea level anomalies in boreal fall (winter) along the west coast of India
- Fall easterly wind anomalies near Sri Lanka force downwelling coastal Kelvin waves that travel quickly to the west coast of India
- Fall eastern equatorial upwelling signals travel more slowly through the interior Bay of Bengal, reaching the Indian west coast in winter

Supporting Information:

- Supporting Information S1

Correspondence to:

I. Suresh,
isuresh@nio.org,
isuresh.nio@gmail.com

Citation:

Suresh, I., Vialard, J., Lengaigne, M., Izumo, T., Parvathi, V., & Muraleedharan, P. M. (2018). Sea level interannual variability along the west coast of India. *Geophysical Research Letters*, *45*, 12,440–12,448. <https://doi.org/10.1029/2018GL080972>




Received 18 OCT 2018

Accepted 13 NOV 2018

Accepted article online 16 NOV 2018

Published online 29 NOV 2018

Sea Level Interannual Variability Along the West Coast of India

I. Suresh¹ , J. Vialard² , M. Lengaigne^{2,3} , T. Izumo^{2,3} , V. Parvathi¹ ,
and P. M. Muraleedharan¹

¹CSIR-National Institute of Oceanography (CSIR-NIO), Dona Paula, Goa, India, ²LOCEAN-IPSL, Sorbonne Université (UPMC, Univ Paris 06)-CNRS-IRD-MNHN, Paris, France, ³Indo-French Cell for Water Sciences, IISc-NIO-IITM-IRD Joint International Laboratory, CSIR-NIO, Dona Paula, Goa, India

Abstract Interannual sea level anomalies (SLA), and the related thermocline variations, along the west coast of India (WCI) strongly impact the ecosystems, fisheries, and potentially the monsoon rainfall. Here we investigate the mechanisms driving the WCI interannual SLA using a linear continuously stratified ocean model, which realistically simulates the leading northern Indian Ocean SLA mode associated with the Indian Ocean Dipole (IOD). During, for example, positive IOD events, easterly wind anomalies near Sri Lanka in late summer and fall force downwelling coastal Kelvin waves, which induce positive WCI SLA within days. Meanwhile, equatorial easterlies force upwelling Kelvin waves that travel to WCI through the Bay of Bengal coastal waveguide. Part of this opposite signal also transits slowly through the Bay of Bengal interior as Rossby waves, eventually yielding negative SLA along the WCI in winter. The WCI SLA thus shifts from positive in fall to negative in winter during positive IOD events.

Plain Language Summary The Indian Ocean Dipole (IOD) is the leading mode of Indian Ocean climate variability and is associated with anomalous winds over the equatorial Indian Ocean. A recent work has demonstrated that IOD events could strengthen or inhibit the upwelling of poorly oxygenated waters along the west coast of India (WCI). Such an upwelling impacts oxygen distribution in the upper layers and can thus have adverse effects on ecosystem and fisheries. Here we explain the mechanisms linking the IOD to upwelling along the WCI. IOD zonal winds in the central equatorial Indian Ocean produce two opposite signals on WCI. One that travels fast, directly up the WCI during summer and fall. But another opposite-polarity signal follows equator and Bay of Bengal rim—a part of which transits slowly through the Bay of Bengal interior, eventually reaching the WCI and flipping the sign of sea level anomalies there in winter.

1. Introduction

The west coast of India (WCI) experiences a seasonal, coastal upwelling, peaking in boreal fall (Schott & McCreary, 2001). Enhanced productivity during this period strongly supports regional fisheries (Banse, 1959), making it important from a socioeconomical viewpoint. This has motivated research on the mechanisms responsible for this seasonal upwelling. Early observational studies (Banse, 1968; Sharma, 1968) noticed a mismatch between upwelling and local winds, suggesting a strong influence of remote forcing. Modeling studies later highlighted significant remote contributions from seasonal winds in the Bay of Bengal (BoB/Bay), with signals from BoB propagating around southern tip of India to the WCI as coastal Kelvin waves (McCreary et al., 1993; Shankar et al., 2002). Suresh et al. (2016) further demonstrated that seasonal wind variations in a small region near southern tip of India and Sri Lanka (STIP region) drive a large fraction (60%) of the WCI sea level seasonal cycle and hence of the upwelling intensity since the sea level variability is a good proxy of thermocline depth variations (Shankar, 2000).

The WCI interannual sea level variability has received considerably less attention than seasonal variability, partly because of its relatively weaker amplitude (Figure S1). Parvathi et al. (2017) however demonstrated that this weak WCI variability, when it combines with the shallowest thermocline in fall (peak upwelling), can have strong socioeconomic impacts. Beyond modulating intensity of seasonal upwelling and the associated productivity, WCI fall interannual sea level anomalies (SLA) modulate occurrence of coastal anoxic (complete depletion of oxygen) events (Parvathi et al., 2017), which have tremendous consequences on fisheries and ecosystems (Naqvi et al., 2000, 2009). The Arabian Sea indeed hosts one of the three major open-ocean Oxygen Minimum Zones globally, resulting from high oxygen consumption associated with

remineralization of sinking organic matter in this highly productive region, and relatively poor ventilation of subsurface layers (Resplandy et al., 2012). The seasonal upwelling brings these hypoxic waters to the wide WCI continental shelf to form the largest natural coastal hypoxic system in the world ocean during fall (Naqvi et al., 2000). The hypoxic conditions become more severe during some years, leading to coastal anoxia, with deleterious impacts on ecosystem and fisheries (Naqvi et al., 2009).

In addition to these strong biological impacts, interannual SLA along the WCI may also have important consequences for the regional climate. The WCI SLAs propagate westward as Rossby waves into the south-eastern Arabian Sea (Shankar & Shetye, 1997; Suresh et al., 2016), where they induce thermocline-depth perturbations, hence potentially influencing local sea surface temperature and thus monsoon rainfall. For instance, the southeastern Arabian Sea is home to a *mini warm pool* in spring that influences both Indian summer monsoon onset date and rainfall (Durand et al., 2004; Masson et al., 2005; Vinayachandran et al., 2007), thereby impacting livelihood of more than one billion inhabitants of the Indian subcontinent.

These strong socioeconomic impacts call for a thorough analysis of interannual sea level variations along the WCI. However, most past studies focused on the BoB (Aparna et al., 2012), where the SLA interannual variability is stronger than that along the WCI (Figure S1b in the supporting information). Clarke and Liu (1994) were the first to suggest that remote equatorial wind forcing could induce coherent interannual SLAs along the 8000-km stretch of the northern Indian Ocean coast. Equatorial zonal wind variations indeed drive equatorial Kelvin waves. Upon reflecting into Rossby waves at the Sumatra coast, part of the impinging wave energy propagates around BoB rim as coastal Kelvin waves and into the BoB interior as Rossby waves, a pathway similar to that at seasonal timescale (Shankar et al., 2002). Han and Webster (2002) further demonstrated that remote equatorial forcing dominates interannual SLA in the eastern BoB, while local and remote equatorial forcing contribute equally in the western BoB.

Aparna et al. (2012) further pointed out that the BoB interannual SLA variations largely co-occur with the two main interannual climate modes affecting the Indian Ocean (Schott et al., 2009): the Indian Ocean Dipole (IOD; Saji et al., 1999; Webster et al., 1999) and the El Niño-Southern Oscillation (ENSO), which influences the Indian Ocean through atmospheric teleconnection (Klein et al., 1999). A positive IOD induces negative SLA in the BoB during April–December, with a peak in fall (Aparna et al., 2012). Due to the tendency of ENSO to trigger IOD (Annamalai et al., 2003), it is difficult to clearly attribute these sea level variations to either ENSO or IOD influence. Several studies used partial correlation techniques to isolate intrinsic SLA signals associated with ENSO and IOD (Currie et al., 2013; Rao & Behera, 2005; Yu et al., 2005). They found that ENSO-induced wind variations are weaker and further south relative to those associated with IOD, so that the IOD dominates oceanic interannual variability in the northern Indian Ocean.

Parvathi et al. (2017) is to our knowledge the only study that investigated the WCI interannual thermocline (hence SLA) variability, owing to its strong impact on anoxic events there. They found that the fall IOD-induced easterly wind anomalies near southern tip of India were well correlated with WCI interannual SLA, favoring downwelling anomalies (during positive IOD). They proposed a mechanism, similar to that at seasonal timescale (Suresh et al., 2016), in which the zonal wind-stress variations at southern tip of India force coastal Kelvin waves that travel to the WCI. They have however neither demonstrated it, nor worked out the relative contributions from local winds and remote forcing from STIP, BoB, or equatorial regions. Given their strong societal implications, interannual sea level variations along the WCI need to be thoroughly described and understood. This is the goal of this paper. Section 2 describes our linear ocean model and related sensitivity experiments that allow us to isolate the aforementioned processes. Section 3 describes the IOD influence on the WCI interannual SLA variability and identifies its main remote and local forcing mechanisms. Section 4 summarizes and discusses our main findings.

2. The Model and Methods

We use a modified version of the linear, continuously stratified ocean model of McCreary et al. (1996), which we previously used for studying the northern Indian Ocean intraseasonal sea level variability (Suresh et al., 2013) and sea level seasonal cycle along the WCI (Suresh et al., 2016). Shallow water equations are solved for the first five baroclinic modes at 0.25°-resolution over the Indian Ocean (30°S to 30°N, 30°E to 110°E), with a coastline derived from 200-m isobaths. The model solution is obtained as the sum of these modes (summing first 20 modes gives similar results, not shown). The model is forced with daily TropFlux wind-stress

(Praveen Kumar et al., 2013) anomalies relative to long-term mean over 1979–2013. This solution is referred to as the control (CTL) experiment. The model reproduces very well the basin-scale sea level variability in the northern Indian Ocean at intraseasonal (Suresh et al., 2013) and seasonal (Suresh et al., 2016) timescales. Its performance at interannual timescale will be assessed in section 3.1.

Arabian Sea (local) wind forcing and remote forcing from the equatorial, BoB, and STIP regions can all influence the WCI SLA variability. Each of those contributions can further be decomposed into that resulting from alongshore forcing at the coast and that from wind-stress curl in the interior ocean. The sensitivity experiments and decomposition method used to separate these processes are the same as in Suresh et al. (2016), and are further described in the supporting information. The pathways of each of those signals, and the associated forcing hotspots, will be detailed in section 3.2. Our results are not very sensitive to other reasonable choices of model parameters or dampers used in sensitivity experiments (not shown).

Interannual signals are obtained by applying a band-pass filtering with cutoff period of 150 days to 7 years, after subtracting mean seasonal cycle and detrending 1979–2013 time series. The interannual CTL SLA is validated against AVISO merged multisatellite delayed mode product. These observations include effects of mesoscale eddies in, for example, western BoB or Arabian Sea (Chelton et al., 2011), unlike our linear model. We isolate large-scale interannual SLA signals in the Indian Ocean north of 20°S using empirical orthogonal function (EOF) analysis. In order to relate this signal to climate variability associated with IOD or ENSO, we respectively use Dipole Mode Index (DMI) averaged over September–November (SON; the peak season of IOD) and Multivariate ENSO Index averaged over November–January (NDJ; the peak season of ENSO), normalized by their respective standard deviations.

3. Origin and Processes of WCI Interannual Sea Level Variability

3.1. The IOD Influence

Figure 1 displays the first EOF (EOF1) spatial pattern and principal component (PC1) from CTL and observations. The EOF1 is well separated from higher-order modes in both model and observations: It indeed explains 64% (53%) of total SLA variance in CTL (observations), while second mode explains only 10% (9%). The overestimated percentage of explained variance in model compared to that in observations results from linearity of the model that does not simulate mesoscale eddies, while observed SLA contains many eddies throughout the basin (Chelton et al., 2011). Apart from that, there is a remarkable agreement between modeled and observed leading EOF patterns (Figures 1a and 1b, pattern correlation of 0.89). Figures 1a and 1b also display the wind stresses associated with this leading mode of interannual SLA (obtained through linear regression of interannual wind-stress anomalies onto PC1). The model and observations both indicate that the leading mode of interannual SLA in the Indian Ocean is associated with equatorial zonal wind-stress anomalies. We will hereon describe results for the above patterns of SLA and winds, although our analysis is equally valid for opposite SLA and wind polarities. These easterly wind-stress anomalies induce upwelling Kelvin wave response in the eastern equatorial Indian Ocean, with one part of the signal propagating into northern Indian Ocean coastal waveguide as coastal Kelvin wave that can be tracked all the way to the Sri Lankan coast (Figures 1a and 1b). The equatorial easterly anomalies also induce downwelling equatorial Rossby wave response to the west. Due to asymmetric wind forcing around the equator (10°S–6°N), the SLA response is more pronounced in the southern hemisphere. The model underestimates this positive SLA response but compares reasonably well with observations in the northern hemisphere, including the WCI. Finally, temporal variations associated with this leading mode are strikingly similar between modeled and observed PC1, with a 0.97 correlation (Figure 1c).

The leading SLA mode and associated wind signals (Figures 1a and 1b) are reminiscent of those associated with a positive IOD (Murtugudde et al., 2000; Webster et al., 1999). As noted in introduction, there is a tendency for ENSO to trigger IOD (Annamalai et al., 2003), making it difficult to isolate intrinsic SLA signals associated with IOD (i.e., IOD occurring without ENSO forcing) from those associated with ENSO (i.e., driven by ENSO teleconnections, when they fail to trigger IOD). Previous studies (Currie et al., 2013; Rao & Behera, 2005; Yu et al., 2005) have however demonstrated that most of the northern Indian Ocean interannual SLA and thermocline variations are mainly driven by IOD-related wind signals. In line with those studies, both observed and modeled SON PC1 exhibit higher correlation with SON DMI (~0.95) than with NDJ

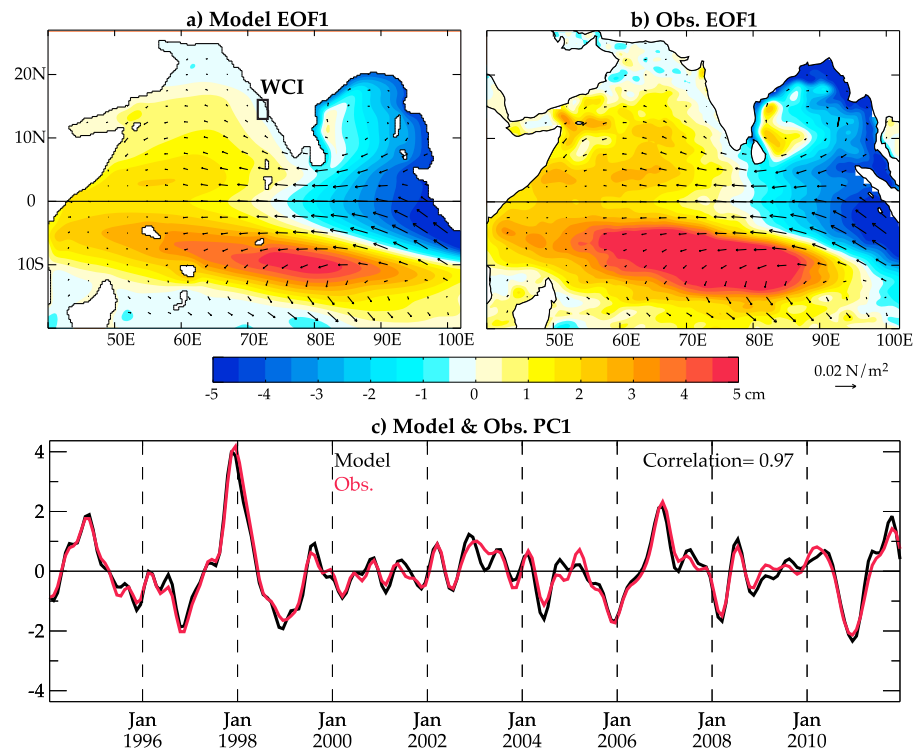


Figure 1. Leading EOF of interannual SLAs in the Indian Ocean from (a) model CTL experiment and (b) satellite-altimeter observations; (c) associated normalized PC1 (model [black], observations [red]). The associated wind-stress anomalies on panels (a) and (b) are obtained through regression of interannual wind stresses onto normalized PC1. The black box, which is representative of the WCI and used in Figure 3, is marked on panel (a).

Multivariate ENSO Index (0.81; Figure S2), corroborating that EOF1 is associated with IOD intrinsic variability, rather than ENSO.

The typical temporal evolution of IOD-related SLA patterns can be obtained through a lead/lag regression onto SON DMI. We will focus on describing those typical signals in October (Figure 2a; during IOD peak, also representative of IOD growth in summer) and in February (Figure 2f; after IOD termination) as these two periods display opposite SLA along the WCI. Positive IODs are associated with positive SLAs along the WCI in October (Figure 2a) and negative SLAs in February (Figure 2f). The October SLA pattern is very similar to that on Figure 1a described above. By February, IOD-induced equatorial easterly wind anomalies have largely disappeared. Negative SLA signals persist over the entire eastern Indian Ocean, including in the BoB and along the WCI. In the next subsection, we will use dedicated model sensitivity experiments to understand the dynamics involved in this evolution, with a specific focus on the WCI, where SLAs have strong societal impacts.

3.2. Processes of IOD-Induced Interannual Sea Level Variations

We isolate contributions from various forcing regions to interannual SLA anomalies in the northern Indian Ocean, or specifically along WCI, following the same strategy as in Suresh et al. (2016; more details in the supporting information). The pathways linking each forcing region to WCI are shown schematically on Figure 2. We will briefly remind those pathways. Equatorial zonal winds trigger Kelvin waves that travel to the eastern boundary, where a part of the energy gets reflected back as equatorial Rossby waves (light-blue dashed arrows at lowest latitude on Figure 2c) and another part propagates into the BoB as coastal Kelvin waves. Part of this BoB signal follows the BoB rim and further propagates around Sri Lanka to the WCI as coastal Kelvin waves (light-blue continuous arrow on Figure 2c). A fraction of coastal Kelvin-wave energy on the eastern BoB rim is radiated westward as Rossby waves (light-blue dashed arrows on Figure 2c). This signal takes considerably longer time to reach the Indian east coast than Kelvin-wave signal that follows the coastal waveguide. For example, a long nondispersive first mode baroclinic Rossby wave would take ~ 60 (~ 100) days to

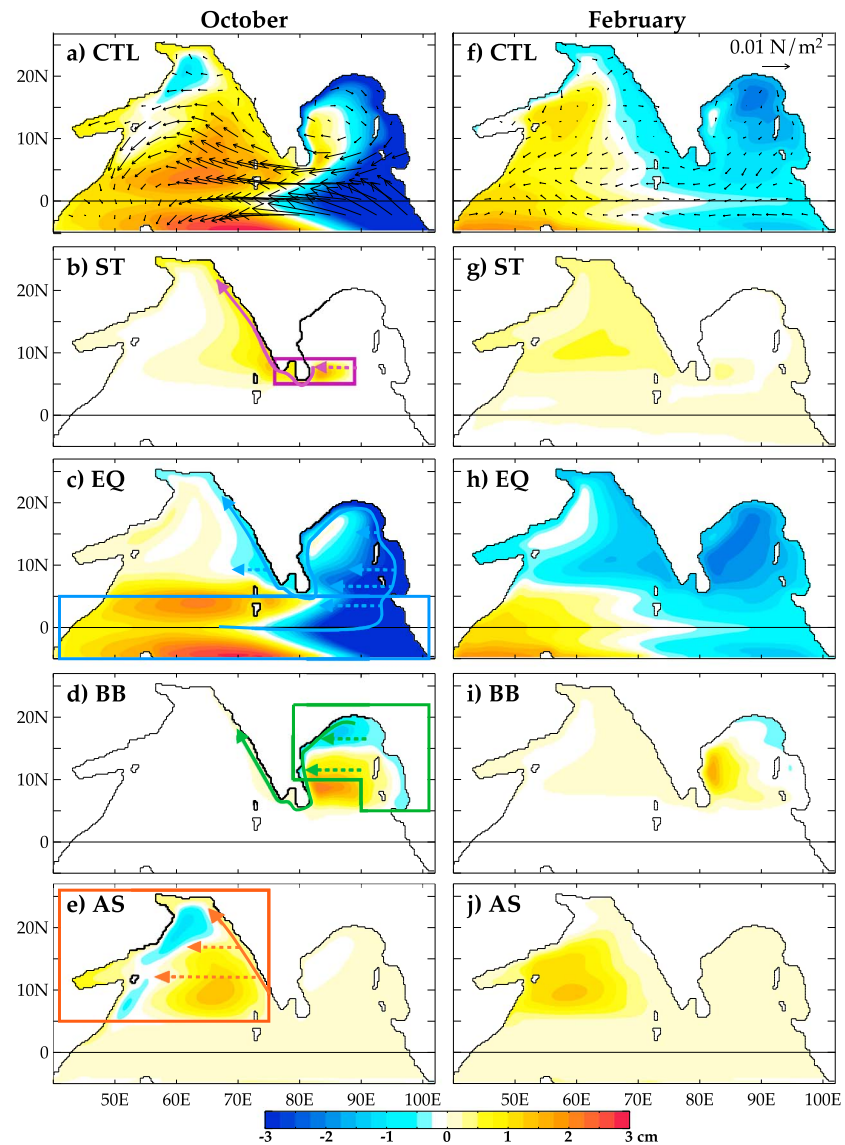


Figure 2. Typical IOD basin-scale SLAs and contributions from forcing in various regions, obtained as lead/lag regressions of the (a–e) October and (f–j) February interannual anomalies onto normalized SON-averaged DMI for (a and f) CTL SLA and wind stresses and decomposition of CTL SLA into (b and g) STIP forcing or ST process (purple box and arrows); (c and h) equatorial forcing or EQ process (light blue); (d and i) BoB forcing or BB process (green); and (e and j) Arabian Sea forcing or AS process (red). The ST, EQ, BB, and AS contributions add up to CTL, owing to model linearity. Arrows symbolize the pathways of equatorial and coastal Kelvin waves (continuous) and Rossby waves (dashed).

cross the BoB at 8°N (10°N; Figure S4), while a first baroclinic mode coastal Kelvin wave (with a typical speed of 2.5 m/s) would take less than 20 days to travel the ~4,000-km distance separating the Andaman Sea from Sri Lanka along the shelf break. These coastal Kelvin waves then take less than a week to travel from Sri Lanka to the WCI northern end. These signals associated with remote equatorial forcing will be referred to as EQ.

BoB wind variations force signals that include coastal Kelvin waves resulting from alongshore wind variations (ABB; green continuous line on Figure 2d) and Rossby waves induced by Ekman pumping in the BoB interior (IBB; green dashed line on Figure 2d; McCreary et al., 1996; Suresh et al., 2016). The above signals associated with BoB forcing will be named BB.

As demonstrated by Suresh et al. (2016) for the seasonal timescale, STIP wind variations can also induce coastal Kelvin waves, either directly through alongshore forcing (AST; purple continuous line on Figure 2b)

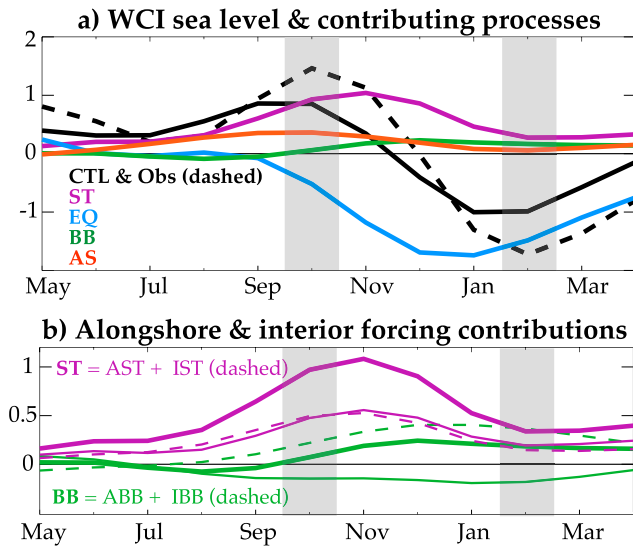


Figure 3. Typical IOD SLA along WCI and contributing processes, obtained as lead/lag regressions of interannual SLA (cm) on WCI box (Figure 1a) to normalized SON-averaged DMI for (a) CTL (continuous black), with its observed counterpart (dashed black), and its decomposition into ST (purple), EQ (light blue), BB (green), and AS (red) processes. (b) BB and AS processes (thick continuous) are further decomposed into alongshore (thin continuous) and interior wind-stress curl (thin dashed) forcing contributions. The gray vertical strips mark October and February, for which basin-scale patterns are displayed on Figure 2.

ling coastal Kelvin waves (i.e., AST). Meanwhile, the poleward decrease of easterly wind anomalies leads to strong negative wind-stress curl (Figures 2a and S3d) east of Sri Lanka, inducing downwelling Rossby waves that reach the Sri Lankan coast within 1–2 weeks and trigger downwelling coastal Kelvin waves (i.e., IST). The resulting downwelling ST signals (Figure 2b) propagate northward along the WCI as coastal Kelvin waves. AST and IST signals are in phase and both contribute nearly equally to ST (Figure 3b). While the peak of ST forcing (Figures S3c and S3d) coincides with the typical IOD peak in October, its contribution along the WCI peaks in November (Figure 3), as the ocean is an integrator of wind forcing. The ST contribution to WCI starts decreasing in December (Figure 3), coinciding with the IOD termination and disappearance of STIP wind anomalies (Figures S3e and S3f).

EQ is due to equatorial easterlies during a positive IOD, inducing upwelling in the eastern equatorial Indian Ocean, with part of this signal propagating into the BoB coastal waveguide as coastal Kelvin waves (Figure 2c). Coastal Kelvin wave takes ~25 days to travel the ~5,500 km of coastal waveguide between the eastern Indian Ocean and the WCI (at 10°N), with the typical speed (2.5 m/s) of first baroclinic mode. Part of the upwelling EQ signal thus reaches the WCI within a month and interferes destructively with downwelling ST signal (Figures 2b, 2c, and 3a), thereby decreasing CTL SLA during November. Meanwhile, part of the EQ negative SLA on the BoB eastern rim radiates westward into interior Bay as upwelling Rossby waves (Figure 2c). As noted earlier, Rossby waves take ~2 months at 8°N to ~6 months northward of 14°N to cross the Bay (Figure S4). This explains why the EQ contribution to WCI peaks in December–February (roughly 2–3 months after the peak of IOD equatorial wind anomalies) and dominates the CTL SLA after ST has receded. EQ continues to contribute to CTL SLA until March–April when equatorial wind anomalies have completely receded (Figures 2f and S3g). The slow propagation of this fraction of the EQ signal through interior BoB as Rossby waves thus explains the delayed EQ contribution to CTL negative SLA along the WCI during winter and the following spring.

The AS and BB processes contribute only weakly to WCI SLA. AS is due to the relatively weak IOD-induced WCI alongshore forcing (Figure 2a; poleward weakening of WCI winds up to 15°N, yielding weak positive SLA on Figures 2e and 3a; nonnegligible only during late summer and fall). The BB contribution is even weaker due to opposing contributions from alongshore (ABB) and interior (IBB) BoB forcing (Figure 3b). The anomalous

or indirectly through Rossby waves forced by strong wind-stress curl east of Sri Lanka (IST; dashed purple line on Figure 2b). We will name this process ST. We will also isolate the effect of Arabian Sea wind forcing (AS), which reduces to local alongshore forcing for WCI (wind-stress curl forces Rossby waves further west in the interior Arabian Sea).

We will now examine how the aforementioned processes contribute to the IOD-induced interannual SLA along the WCI (estimated as lead/lag regression of CTL interannual SLA onto SON-averaged DMI; regression onto SON-averaged PC1 gives similar results). Figure 2 presents maps of these process contributions for October and February, while Figure 3 displays time series of those contributions to WCI SLA during a typical positive IOD. ST and EQ are the dominant processes driving the IOD-related WCI interannual SLA (plus a weaker AS contribution almost in phase with ST, nonnegligible in late summer and early fall; Figure 3a). During a positive IOD, the WCI SLA sign changes from positive during late summer and fall to negative during winter both in CTL and observations (Figure 3a). ST induces positive SLA along the WCI, with its contribution peaking in October–November (Figure 3a). In contrast, EQ induces negative SLA that peaks later in December–January (Figure 3a). The trade-off between positive ST and delayed negative EQ SLAs determines the WCI SLA change of sign from boreal fall to winter.

During late summer and fall, equatorial easterly wind-stress anomalies during a positive IOD extend off the equator to ~10°N (Figure 2a), leading to strong alongshore forcing in the STIP region (Figures S3c and S3d). The resulting northward Ekman transport towards the coast induces downwelling

anticyclonic wind circulation in BoB (Figure 2a) indeed yields negative wind-stress curl (Figure S3d) that forces downwelling IBB signals in the southern BoB (Figure 2d). The above anticyclonic circulation (Figure 2a) is also associated with upwelling-favorable alongshore winds all around the BoB rim, especially along the northwestern boundary (Figure S3d), yielding negative ABB signals (Figure 2d). These two opposite signals result in overall weak BB remote forcing contribution to WCI SLA during fall and winter (Figure 3b).

4. Summary and Discussion

Parvathi et al. (2017) recently demonstrated that IOD events could modulate the thermocline (and oxycline) depth anomalies along the WCI during fall and thus favor or inhibit anoxia along the WCI. It is therefore important to understand the processes by which IOD influences the WCI. Parvathi et al. (2017) hypothesized a key role of zonal wind variations near the southern tip of India, as that previously demonstrated for the seasonal cycle (Suresh et al., 2016) but did not demonstrate it. Here we use a linear ocean model to explore the main processes that influence interannual SLA (and hence thermocline/oxycline variations) along the WCI during an IOD event. The leading mode of interannual SLA variability in the Indian Ocean is associated with the IOD and is very well reproduced by our model. A typical positive IOD is associated with positive SLAs off the WCI in late summer and fall, and negative anomalies in following winter and spring. Equatorial easterly wind anomalies typical of positive IODs extend sufficiently northward to STIP region to trigger downwelling coastal Kelvin waves, which dominate WCI SLA during late summer and fall. Part of the upwelling Kelvin waves driven by equatorial easterlies propagates into BoB and then transits slowly (2–6 months) as westward Rossby waves through BoB interior. At the western BoB rim, those Rossby waves excite upwelling coastal Kelvin waves, which bend around Sri Lanka and propagate to WCI. This delayed negative signal, which has so far not been discussed in the literature, dominates the WCI SLA during the winter and spring following positive IOD events.

Aparna et al. (2012) had remarked that negative IODs were associated with smaller SLAs than their positive counterpart in BoB. Along the same lines, Parvathi et al. (2017) reported an asymmetric influence of positive and negative IOD events on WCI oxycline/thermocline variations, with positive IODs suppressing anoxia, while negative IODs having a less systematic impact. They attributed this asymmetry to weaker wind anomalies near southern tip of India during negative IODs, in relation with the skewed nature of IOD itself (Saji & Yamagata, 2003). Our model allows us to further investigate the processes responsible for this asymmetry (Figure S5). The ST contribution is indeed weaker for negative than for positive IODs, as hypothesized by Parvathi et al. (2017), but only by ~20%, while the total SLA is weaker by ~60%. Our decomposition further shows that BB contribution is almost negligible or negative for negative IOD, also explaining a large part of the asymmetry. On the other hand, the EQ contribution remains nearly symmetric, suggesting that equatorial zonal wind-stress anomalies have roughly similar magnitudes for positive and negative IODs, but they extend further north towards STIP and BoB during positive IODs.

Previous studies that investigated the mechanisms of interannual SLA variations in the northern Indian Ocean (Aparna et al., 2012; Clarke & Liu, 1994; Han & Webster, 2002) focused on BoB. Though our study focuses on WCI, we discuss the results for BoB (Figures 2 and S6a and S6b) for consistency with those studies. All those studies emphasized the importance of remote equatorial forcing for BoB interannual SLA. Han and Webster (2002) showed that equatorial forcing dominates the SLA variability along BoB eastern rim. We find that eastern BoB CTL SLA is entirely due to EQ (Figure S6a). They further found a growing influence of BoB forcing counterclockwise around the Bay, as we do. At the east coast of India, for instance, SLA interannual variability is still dominated by EQ, but with a nonnegligible contribution from BB (Figure S6b). This good agreement between our study and the previous ones for BoB further strengthens confidence in our results for the WCI.

As noted in section 1, SST variations in southeastern Arabian Sea could influence rainfall over India. It is hence worth examining the mechanisms contributing to SLA variability in this region, as those SLAs can influence SST through thermocline feedback and advection associated with passing planetary waves. Southeastern Arabian Sea is downstream along the path of Rossby waves radiated at low latitudes from the WCI (Shankar & Shetye, 1997; Suresh et al., 2016), and hence, the SLA evolution during IOD and the underlying processes (Figure S6c) are very similar to those along the WCI (Figure 3a), with slightly higher contribution from interior Arabian Sea forcing (Figures 2e, 2j, and S6c) as could be expected. A positive IOD thus

induces positive SLA in late summer and fall and negative SLA during the following winter and spring in southeastern Arabian Sea. This modeling result is in line with the XBT observations of strong negative subsurface temperature anomalies in this region from December 2006 to summer 2007 (Gopalakrishna et al., 2010), in both timing and sign, following the strong positive IOD in fall 2006. Besides its potential instantaneous impact on late summer rainfall, the delayed IOD influence could also potentially modulate subsurface conditions in the *Arabian Sea mini-warm pool* (Vinayachandran et al., 2007) in the following spring, which could in turn feedback onto Indian summer monsoon characteristics. This would be further investigated in a future study.

Acknowledgments

Authors thank Director, CSIR-NIO. I. S. thanks Neetu and Sadhvi and acknowledges financial support from ESSO-INCOIS/MoES (HOOFS), NRB/DRDO, and CSIR, New Delhi. J. V., M. L., and T. I. acknowledge financial support from Institut de Recherche pour le Développement (IRD) and CNES-Altika project. This work was done while M. L. and T. I. were visiting scientists at CSIR-NIO supported by IRD funding. J. V. acknowledges IRD for supporting regular visits to CSIR-NIO and CSIR-NIO for *Adjunct Scientist*. V. P. acknowledges CSIR senior research fellowship. Authors thank the reviewers for their constructive comments. A more detailed discussion can be found in the supporting information (Locarnini et al., 2010; Smith & Sandwell, 1997). The manuscript uses Tropflux wind stresses from www.incois.gov.in/tropflux/, sea level observations from www.aviso.oceanobs.com/fr/accueil/index.html, Dipole Mode Index from www.jamstec.go.jp/frcgc/research/d1/iod/DATA/dmi.monthly.txt, and Multivariate ENSO Index from www.esrl.noaa.gov/psd/enso/mei/table.html. This is NIO contribution 6313.

References

- Annamalai, H., Murtugudde, R., Potemra, J., Xie, S. P., Liu, P., & Wang, B. (2003). Coupled dynamics over the Indian Ocean: Spring initiation of the zonal mode. *Deep-Sea Research Part II: Topical Studies in Oceanography*, *50*(12-13), 2305–2330. [https://doi.org/10.1016/S0967-0645\(03\)00058-4](https://doi.org/10.1016/S0967-0645(03)00058-4)
- Aparna, S. G., McCreary, J. P., Shankar, D., & Vinayachandran, P. N. (2012). Signatures of Indian Ocean Dipole and El Niño–Southern Oscillation events in sea level variations in the Bay of Bengal. *Journal of Geophysical Research*, *117*, C10012. <https://doi.org/10.1029/2012JC008055>
- Banse, K. (1959). On upwelling and bottom-trawling off the south west coast of India. *Journal of the Marine Biological Association of India*, *1*, 33–49.
- Banse, K. (1968). Hydrography of the Arabian Sea shelf of India and Pakistan and effects on demersal fishes. *Deep Sea Research and Oceanographic Abstracts*, *15*(1), 45–79. [https://doi.org/10.1016/0011-7471\(68\)90028-4](https://doi.org/10.1016/0011-7471(68)90028-4)
- Chelton, B. D., Schlax, M. G., & Samelson, R. M. (2011). Global observations of nonlinear mesoscale eddies. *Progress in Oceanography*, *91*(2), 167–216. <https://doi.org/10.1016/j.pocean.2011.01.002>
- Clarke, A. J., & Liu, X. (1994). Interannual sea level in the northern and eastern Indian Ocean. *Journal of Physical Oceanography*, *24*(6), 1224–1235. [https://doi.org/10.1175/1520-0485\(1994\)024<1224:ISLITN>2.0.CO;2](https://doi.org/10.1175/1520-0485(1994)024<1224:ISLITN>2.0.CO;2)
- Currie, J. C., Lengaigne, M., Vialard, J., Kaplan, D. M., Aumont, O., Naqvi, S. W. A., & Maury, O. (2013). Indian Ocean Dipole and El Niño/Southern Oscillation impacts on regional chlorophyll anomalies in the Indian Ocean. *Biogeosciences*, *10*(10), 6677–6698. <https://doi.org/10.5194/bg-10-6677-2013>
- Durand, F., Shetye, S. R., Vialard, J., Shankar, D., Shenoi, S. S. C., Ethe, C., & Madec, G. (2004). Impact of temperature inversions on SST evolution in the south-eastern Arabian Sea during pre-summer monsoon season. *Geophysical Research Letters*, *31*, L01305. <https://doi.org/10.1029/2003GL018906>
- Gopalakrishna, V. V., Durand, F., Nisha, K., Lengaigne, M., Boyer, T. P., Costa, J., et al. (2010). Observed intra-seasonal to interannual variability of the upper ocean thermal structure in the southeastern Arabian Sea during 2002–2008. *Deep-Sea Research Part I: Oceanographic Research Papers*, *57*(6), 739–754. <https://doi.org/10.1016/j.dsr.2010.03.010>
- Han, W., & Webster, P. J. (2002). Forcing mechanisms of sea level interannual variability in the Bay of Bengal. *Journal of Physical Oceanography*, *32*(1), 216–239. [https://doi.org/10.1175/1520-0485\(2002\)032<0216:FMOCLI>2.0.CO;2](https://doi.org/10.1175/1520-0485(2002)032<0216:FMOCLI>2.0.CO;2)
- Klein, S. A., Soden, B. J., & Lau, N.-C. (1999). Remote sea surface temperature variations during ENSO: Evidence for a tropical atmospheric bridge. *Journal of Climate*, *12*(4), 917–932. [https://doi.org/10.1175/1520-0442\(1999\)012<0917:RSSTVD>2.0.CO;2](https://doi.org/10.1175/1520-0442(1999)012<0917:RSSTVD>2.0.CO;2)
- Locarnini, R. A., Mishonov, A. V., Antonov, J. I., & Boyer, T. P. (2010). In S. Levitus (Ed.), *World ocean atlas 2009, volume 1: Temperature*, NOAA Atlas NESDIS (Vol. 68, p. 184). Washington, DC: U.S. Government Printing Office.
- Masson, S., Luo, J.-J., Madec, G., Vialard, J., Durand, F., Gualdi, S., et al. (2005). Impact of barrier layer on winter-spring variability of the southeastern Arabian Sea. *Geophysical Research Letters*, *32*, L07703. <https://doi.org/10.1029/2004GL021980>
- McCreary, J. P., Han, W., Shankar, D., & Shetye, S. R. (1996). Dynamics of the East India coastal current. 2. Numerical solutions. *Journal of Geophysical Research*, *101*(C6), 13,993–14,010. <https://doi.org/10.1029/96JC00560>
- McCreary, J. P. Jr., Kundu, P. K., & Molinari, R. L. (1993). A numerical investigation of dynamics, thermodynamics and mixed-layer processes in the Indian Ocean. *Progress in Oceanography*, *31*(3), 181–244. [https://doi.org/10.1016/0079-6611\(93\)90002-U](https://doi.org/10.1016/0079-6611(93)90002-U)
- Murtugudde, R., McCreary, J. P., & Busalacchi, A. J. (2000). Oceanic processes associated with anomalous events in the Indian Ocean with relevance to 1997–1998. *Journal of Geophysical Research*, *105*, 3295–3306.
- Naqvi, S. W. A., Jayakumar, D. A., Narvekar, P. V., Naik, H., Sarma, V. V. S. S., D'Souza, W., et al. (2000). Increased marine production of N₂O due to intensifying anoxia on the Indian continental shelf. *Nature*, *408*(6810), 346–349. <https://doi.org/10.1038/35042551>
- Naqvi, S. W. A., Naik, H., Jayakumar, D. A., Pratihary, A. K., Narvenkar, G., Kurian, S., et al. (2009). Seasonal anoxia over the Western Indian continental shelf. *Geophysical Monograph Series*, *185*, 333–345. <https://doi.org/10.1029/2008GM000745>
- Parvathi, V., Suresh, I., Lengaigne, M., Ethe, C., Vialard, J., Levy, M., et al. (2017). Positive Indian Ocean Dipole events prevent anoxia along the west coast of India. *Biogeosciences*, *14*(6), 1541–1559. <https://doi.org/10.5194/bg-14-1541-2017>
- Praveen Kumar, B., Vialard, J., Lengaigne, M., Murty, V. S. N., McPhaden, M. J., Cronin, M., et al. (2013). TropFlux wind stresses over the tropical oceans: Evaluation and comparison with other products. *Climate Dynamics*, *40*(7-8), 2049–2071. <https://doi.org/10.1007/s00382-012-1455-4>
- Rao, S. A., & Behera, S. K. (2005). Subsurface influence on SST in the tropical Indian Ocean: Structure and inter-annual variability. *Dynamics of Atmospheres and Oceans*, *39*, 103–2135. <https://doi.org/10.1016/j.dynatmoce.2004.10.014>
- Resplandy, L., Lévy, M., Bopp, L., Echevin, V., Pous, S., Sarma, V. V. S. S., & Kumar, D. (2012). Controlling factors of the oxygen balance in the Arabian Sea's OMZ. *Biogeosciences*, *9*, 5095–5109. <https://doi.org/10.5194/bg-9-5095-2012>
- Saji, N. H., Goswami, B. N., Vinayachandran, P. N., & Yamagata, T. (1999). A dipole mode in the tropical Indian Ocean. *Nature*, *401*, 360–363.
- Saji, N. H., & Yamagata, T. (2003). Structure of SST and surface wind variability during Indian Ocean Dipole Mode years: COADS observations. *Journal of Climate*, *16*(16), 2735–2751. [https://doi.org/10.1175/1520-0442\(2003\)016<2735:SOSASW>2.0.CO;2](https://doi.org/10.1175/1520-0442(2003)016<2735:SOSASW>2.0.CO;2)
- Schott, F. A., & McCreary, J. P. (2001). The monsoon circulation of the Indian Ocean. *Progress in Oceanography*, *51*(1), 1–123. [https://doi.org/10.1016/S0079-6611\(01\)00083-0](https://doi.org/10.1016/S0079-6611(01)00083-0)
- Schott, F. A., Xie, S.-P., & McCreary, J. P. Jr. (2009). Indian Ocean circulation and climate variability. *Reviews of Geophysics*, *47*, RG1002. <https://doi.org/10.1029/2007RG000245>
- Shankar, D. (2000). Seasonal cycle of sea level and currents along the coast of India. *Current Science*, *78*(3), 279–288.

- Shankar, D., & Shetye, S. R. (1997). On the dynamics of the Lakshadweep high and low in the southeastern Arabian Sea. *Journal of Geophysical Research*, 102(C6), 12,551–12,562. <https://doi.org/10.1029/97JC00465>
- Shankar, D., Vinayachandran, P. N., & Unnikrishnan, A. N. (2002). The monsoon currents in the north Indian Ocean. *Progress in Oceanography*, 52(1), 63–120. [https://doi.org/10.1016/S0079-6611\(02\)00024-1](https://doi.org/10.1016/S0079-6611(02)00024-1)
- Sharma, G. S. (1968). Seasonal variation of some hydrographic properties of the shelf waters off the west coast of India. *Bulletin of the National Institute of Sciences of India*, 38, 263–275.
- Smith, W. H. F., & Sandwell, D. T. (1997). Global sea floor topography from satellite altimetry and ship depth soundings. *Science*, 277(5334), 1956–1962. <https://doi.org/10.1126/science.277.5334.1956>
- Suresh, I., Vialard, J., Izumo, T., Lengaigne, M., Han, W., McCreary, J., & Muraleedharan, P. M. (2016). Dominant role of winds near Sri Lanka in driving seasonal sea level variations along the west coast of India. *Geophysical Research Letters*, 43, 7028–7035. <https://doi.org/10.1002/2016GL069976>
- Suresh, I., Vialard, J., Lengaigne, M., Han, W., McCreary, J., Durand, F., & Muraleedharan, P. M. (2013). Origins of wind-driven intraseasonal sea level variations in the North Indian Ocean coastal waveguide. *Geophysical Research Letters*, 40, 5740–5744. <https://doi.org/10.1002/2013GL058312>
- Vinayachandran, P. N., Shankar, D., Kurian, J., Durand, F., & Shenoi, S. S. C. (2007). Arabian Sea mini warm pool and the monsoon onset vortex. *Current Science*, 93(2), 203–214.
- Webster, P. J., Moore, A. M., Loschnigg, J. P., & Leben, R. R. (1999). Coupled oceanic–atmospheric dynamics in the Indian Ocean during 1997–98. *Nature*, 401(6751), 356–360. <https://doi.org/10.1038/43848>
- Yu, W., Xiang, B., Liu, L., & Liu, N. (2005). Understanding the origins of interannual thermocline variations in the tropical Indian Ocean. *Geophysical Research Letters*, 32, 24706. <https://doi.org/10.1029/2005GL024327>